

# Measuring Gravitational Redshifts in Galaxy Clusters

Nick Kaiser

*Institute for Astronomy, University of Hawaii*

10 August 2018

## ABSTRACT

Wojtak *et al* have stacked 7,800 clusters from the SDSS survey in redshift space. They find a small net blue-shift for the cluster galaxies relative to the brightest cluster galaxies, which agrees quite well with the gravitational redshift predicted from GR. Zhao *et al.* have pointed out that, in addition to the gravitational redshift, one would expect to see transverse Doppler (TD) redshifts, so  $\langle \delta z \rangle = -\langle \Phi \rangle + \langle \beta^2 \rangle / 2$  with  $\beta$  the 3D source velocity in units of  $c$ , and that these two effects are generally of the same order. Here we show that there are other corrections that are also of the same order of magnitude. The fact that we observe galaxies on our past light cone results in a bias such that more of the galaxies observed are moving away from us in the frame of the cluster than are moving towards us. This causes the observed average redshift to be  $\langle \delta z \rangle = -\langle \Phi \rangle + \langle \beta^2 \rangle / 2 + \langle \beta_x^2 \rangle$ , with  $\beta_x$  is the line of sight velocity. That is if we average over galaxies with equal weight. If the galaxies in each cluster are weighted by their fluence, or equivalently if we do not resolve the moving sources, and make an average of the mean redshift giving equal weight per photon, the observed redshift is  $\langle \delta z \rangle = -\langle \Phi \rangle - \langle \beta^2 \rangle / 2$ , so the kinematical effect is then opposite to the usual transverse Doppler effect. In the WHH experiment, the weighting is a step-function because of the flux-limit for inclusion in the spectroscopic sample and the result is different again, and depends on the details of the luminosity function and the SEDs of the galaxies. Including these effects substantially modifies the blue-shift profile. We show that in-fall and out-flow have very small effect over the relevant range of impact parameters but out-flow becomes significant and needs to be taken into account for measurements on larger scales.

**Key words:** Cosmology: observations; galaxies: clusters: general

## 1 INTRODUCTION

Wojtak, Hansen and Hjorth (2011, hereafter WHH) have measured the gravitational redshift effect in clusters of galaxies. They stacked 7,800 massive clusters selected from the GMBCG cluster sample (Hao, J., *et al.*, 2010) derived from from the SDSS DR7 survey data (Abazajian *et al.*, 2009) in redshift space, using coordinates of the brightest cluster galaxy (BCG) as the origin. They fit the cluster-frame redshift distributions, determined at a range of impact parameters, to a linear ramp to describe the foreground and background galaxies plus a quasi-Gaussian distribution to describe the cluster, and find that the centres of the cluster components have a small net blue-shift  $\delta z \sim -10 \text{ km s}^{-1}/c$ ; a remarkable achievement since the galaxy clusters have velocity dispersions of order 600 km/s.

A blue-shift would be expected in GR (see e.g. Cappi, 1995) since the light from the BCGs, which are thought to reside close to the centres of clusters, will have climbed out from deeper in the cluster potential well than the light from the majority of the galaxies, and the amplitude of the effect

appears to be broadly consistent with their estimates of the gravitational redshift obtained using a mean cluster mass distribution determined from the observed velocity dispersion.

WHH suggested that the result is in conflict with the predictions of TeVeS modified gravity theory (Bekenstein, 2004). However, agreement with the potential inferred from the kinematics of non-relativistic particles like galaxies is expected in any metric theory of gravity since both gravitational redshifts and particle motions are determined by the time component of the metric; what this type of measurement tests is the validity of the equivalence principle (Will, 2006; Bekenstein and Sanders, 2012; Zhao *et al.*, 2012, hereafter ZPL). This type of observation can, however, provide constraints on theories in which there are long-range non-gravitational interactions between dark matter that augments gravity on cluster scales (e.g. Gradwohl & Frieman, 1992; Gubser & Peebles, 2004; Farrar & Rosen, 2007).

WHH compare the fractional frequency shift with the estimate for  $\langle \Phi \rangle_{r_\perp} / c^2$  where the averaging is along a line of sight with impact parameter  $r_\perp$ . This would be approx-

priate if the light were emitted by non-inertial observers on a rigid, non-rotating, lattice in a state of rest with respect to the cluster. It is also valid, to a good approximation, for observations of the redshift of X-ray lines from heavy ions in the intra-cluster medium (Broadhurst & Scannapieco, 2000). But, as emphasised by ZPL, this is not correct when the light emanates from galaxies that are in free-fall. One way to obtain the observed redshift in this situation is to use local Lorentz boosts to give the Doppler shift between each emitting galaxy and its neighbouring lattice-based observer living in the rest-frame of the cluster (though there are other constructions one could use — see Bunn & Hogg (2009) for an in-depth discussion). If we set up coordinates such that the distant observer lives at positive  $x$ , the energy of a photon in the emitting galaxy's frame relative to the cluster rest-frame is  $E_G = \gamma(1 - \beta_x)E_{\text{RF}}$  where  $\gamma = (1 - \beta^2)^{-1/2}$  and  $\beta = \mathbf{v}/c$  with  $\beta_x$  the component towards the observer, so, up to second order in  $\beta$  the redshift is  $1+z = E_G/E_{\text{RF}} = 1 - \beta_x + \beta^2/2$ . Adding the gravitational redshift difference yields the average redshift, given a phase space density (PSD) for the galaxies  $\rho(\mathbf{r}, \boldsymbol{\beta}, t)$ , of

$$\langle \delta z \rangle = \frac{\int d^3r \int d^3\beta \rho(\mathbf{r}, \boldsymbol{\beta}, t) (-\beta_x + \beta^2/2 - \Phi/c^2)}{\int d^3r \int d^3\beta \rho(\mathbf{r}, \boldsymbol{\beta}, t)}. \quad (1)$$

Note that the redshifts here are all relative redshifts between observers and emitters in the vicinity of the cluster, not the redshift actually observed; i.e.  $1+z = (1+Z_{\text{obs}})/(1+Z_{\text{CL}})$ .

If the cluster is virialised, the PSD will be an even function of velocity so the mean of the line-of-sight velocity  $\beta_x$  will vanish, and one would conclude that the mean redshift difference is

$$\langle \delta z \rangle = \langle z_G - z_{\text{BCG}} \rangle = \langle \beta_G^2 - \beta_{\text{BCG}}^2 \rangle / 2 - \langle \Phi_G - \Phi_{\text{BCG}} \rangle / c^2 \quad (2)$$

where now, following ZPL, allowance is made for the fact that the BCG will, in general, not be at rest at the centre of the cluster. Thus there is a positive contribution to the redshift, the transverse Doppler (TD) effect, that is opposite in sign to the gravitational redshift (GR) effect for rest-frame emitters (it being assumed here that the BCGs are on considerably lower energy orbits than the general cluster population) and, as emphasised by ZPL this effect will, quite generally, be of the same order as the gravitational redshift for a bound system by virtue of the virial theorem.

The point of this paper is to show that there are other corrections of the same order of magnitude. One arises from the fact that we observe the galaxies on our past light cone and this causes a bias such that we see more galaxies moving away from us than moving towards us. We show in §2 that this gives an additional redshift  $\langle \beta_x^2 \rangle$ .

But that is only true if each source galaxy is weighted equally in the averaging. If we apply any weighting based on galaxy luminosity then we also need to allow for the special relativistic beaming effect. In §3 we show that if we do not resolve the internal motions, but make an average that gives equal weight per observed photon, the resulting redshift is just the opposite of the transverse Doppler effect. That beaming and time-dilation would have an effect on gravitational redshift measurements using X-ray observations was noted by Broadhurst & Scannapieco (2000), but in that application it is a much smaller effect so was ignored.

In the WHH experiment the weighting was a step-function imposed by the flux-limit for inclusion in the spec-

troscopic sample. We calculate the effect of this in §4. This turns out to be the dominant kinematic effect.

In §5 we apply these results together with the observed velocity dispersion profile to generate revised predictions for the net effect and compare with the observations.

In §6 we consider the effect of infall and outflow, which we find to have very little impact on the measurements, and in an appendix we develop the formalism for deriving, from numerical or analytical models, the predicted distribution of observed redshifts in order to facilitate a more direct comparison with the current and future observations.

## 2 PHASE SPACE DENSITY ON THE PAST LIGHT-CONE

One might imagine that allowing for the light travel time would be simply a matter of replacing  $\rho(\mathbf{r}, \boldsymbol{\beta}, t)$  in equation (1) by  $\rho(\mathbf{r}, \boldsymbol{\beta}, t = x/c)$ , in which case there would be no effect in the virialised region since for a stable, relaxed, system the PSD is independent of time. We are choosing the origin of time here to be the time the light we observe left the center of the cluster.

But this is not correct. While the PSD is invariant under Lorentz boosts and also along the trajectories of the particles, it has a non-trivial transformation from rest-frame to light-cone (LC) coordinates:

$$\rho_{\text{LC}}(\mathbf{r}, \boldsymbol{\beta}) = (1 - \beta_x) \rho_{\text{RF}}(\mathbf{r}, \boldsymbol{\beta}). \quad (3)$$

This means that the PSD for a virialised system viewed on the light cone is not an even function of velocity but has a small asymmetry which results in a non-vanishing of the mean of the line of sight component of the velocity.

One way to see how this arises is to consider taking a photograph of a swarm of particles where, in any region of space, there are as many particles moving towards us as away from us. The particles that we will see in a small cubical cell in space are not the same as the particles that occupy the cell at the moment the light passes through the centre of the cell. As the past light cone of the event of our opening the shutter sweeps towards us through the cell it will overtake more particles that are moving away from us than are moving towards us. The result is that more particles in the photograph will have positive radial velocities than negative ones, as was found in a slightly different context by Dunkel et al., 2009. More quantitatively, if we have a pair of particles with the same  $x$ -component of velocity  $\beta_x$  with separation in the rest frame of  $dx$  then on our past light-cone they have a separation  $dx_{\text{LC}} = dx_{\text{RF}}/(1 - \beta_x)$  and so the density (ordinary space density or phase space density) on the light cone gains a factor  $1 - \beta_x$ . Note that this is a purely Newtonian plus light-travel-time effect, and has nothing to do with Lorentz-Fitzgerald length contraction which causes the density of particles to depend on the state of motion of the observer. It is the same effect that causes a runner on a trail to meet more hikers coming the other way than going in the same direction.

This result can easily be verified in the case of a toy model of a particle oscillating back and forth in a 1D parabolic potential well  $\Phi(x) = \omega^2 x^2/2$ . The trajectory is  $x(t) = a \cos(\omega t + \phi)$ , where  $\phi$  is the phase. The velocity in the rest-frame of the potential trough is  $\beta =$

$-(a\omega/c)\sin(\omega t + \phi)$  which, on the light cone  $t = x/c$  is  $\beta = -(a\omega/c)\sin(\omega x/c + \phi) \simeq -(a\omega/c)\sin\phi - (a\omega/c)^2\cos^2\phi$ . The average of first term (over phase, or equivalently over time) vanishes, but the second term is always negative and is just  $-\beta^2$ , and the average agrees with  $\langle\beta\rangle = \int dx \int d\beta \rho(x, \beta)(1 - \beta)\beta / \int dx \int d\beta \rho(x, \beta)(1 - \beta) = -\langle\beta^2\rangle$  with the rest frame PSD an even function of velocity.

For this toy model, and for particles uniformly distributed in phase, the PSD is zero except on a circle in  $(x', \beta)$  space (where  $x' = x\omega/c$  is the dimensionless displacement), and  $\rho(x', \beta, t)$  vanishes except on a cylinder around the  $t$ -axis. When we slice this cylinder on the light cone, the particles also live on a circle, but their density is non-uniform.

A parabolic 1-D potential is not very realistic, but the result is quite general. For particles orbiting in any static potential well, the average of the instantaneous line of sight velocity, either over time for one particle or over phase for a distribution, will average to zero, but the observed velocity will contain an extra term which is the light propagation time  $x/c$  times the acceleration of the particle, and the acceleration and position are anti-correlated in a gravitationally bound system, so this does not average to zero. Since the acceleration is the gradient of the potential, it is guaranteed that the average of the line-of-sight velocity will be of the same order as  $\Phi/c$ .

WHH measured the mean redshift difference for galaxies at a range of projected distances  $r_\perp$  from the cluster center. The appropriate thing to compare with a PSD from a dynamical model or output of a numerical simulation is, with suitable normalisation,

$$\langle\delta z\rangle_{r_\perp} = \int dx \int d^3\beta \rho_{\text{RF}}(\mathbf{r}, \beta, t = x/c)(1 - \beta_x) \times (-\beta_x + \beta^2/2 - \Phi/c^2). \quad (4)$$

In the virialised region, this gives

$$\langle z - z_{\text{BCG}} \rangle = \langle \beta_x^2 - \beta_{x\text{BCG}}^2 \rangle + \langle \beta^2 - \beta_{\text{BCG}}^2 \rangle / 2 - \langle \Phi_{\text{G}} - \Phi_{\text{BCG}} \rangle / c^2. \quad (5)$$

For isotropic orbits, the new term is 2/3 of the size of the TD effect and is of the same sign. Note that the asymmetry in the PSD applies to BCG as well; BCG line of sight velocities will also be biased to be positive with respect to the cluster centre of mass.

### 3 UNRESOLVED SOURCES

The foregoing analysis assumes that the redshift offsets are determined from a catalogue of angular positions and redshifts, thus effectively giving equal weight per galaxy.

But when we cannot resolve the sources, such as when we try to allow for the kinematics of stars in BCGs, or, potentially, for low resolution HI observations of clusters, we are averaging with equal weight per observed *photon*, and this changes the effect.

Consider a source that emits photons of fixed energy  $E = E_0$  isotropically in its rest-frame in a burst as it passes the origin of space moving at velocity  $\beta$  along the  $x$ -axis. Boosting the photon 4-momenta into the 'laboratory frame' (denoted below by primed coordinates) one finds that a distant observer measures an energy  $E(\mu') =$

$E_0/\gamma(1 - \beta\mu') = E_0\gamma(1 + \beta\mu)$  where  $\mu$  is the cosine of the angle between the  $x$ -axis and the photon direction. Comparing the 3-momenta yields  $\mu' = (\beta - \mu)/(1 + \beta\mu)$ , and therefore the Jacobian of the transformation from observed to source-frame solid angles is  $d\mu'/d\mu = 1/\gamma^2(1 + \beta\mu)^2 = (E_0/E)^2$ , and since  $n(\mu')d\mu' = n_0d\mu$ , the density of photons per unit solid angle is  $n(\mu') = n_0(E/E_0)^2 = n_0/\gamma^2(1 - \beta\mu')^2$ . This is the familiar relativistic beaming effect. The energy is a function of lab-frame direction, and one finds that the probability distribution for energy is  $P(E) \propto n(\mu')d\mu'/dE(\mu')$  which is flat from  $E = E_0/\gamma(1 + \beta)$  to  $E = E_0/\gamma(1 - \beta)$ , and zero otherwise.

This is the probability distribution for random direction to the observer, or, equivalently, the probability distribution for a single observer viewing radiation from sources at the origin moving in random directions. It is also the same distribution one would find for a particle oscillating back and forth in a box, or for the emission from particles in a region of space if they are moving in randomly oriented directions though all at the same speed. The mean photon energy is readily found to be  $\langle E \rangle = \int dE EP(E) = \gamma E_0$ ; a result that could have been anticipated since whatever rest-mass  $\delta m_0$  the source used to create the radiation has energy in the lab-frame  $\gamma\delta m_0 c^2$ .

For a distribution of velocities we need to allow for the time-dilation effect: if the sources are identical and all emitting photons at a fixed rate in the frame, the interval between emission events in the observer-frame will be longer by a factor  $\gamma$ , so the number of photons observed per unit time from sources with gamma factor  $\gamma$  is  $d\dot{n}(\lambda) \propto P(\gamma)d\gamma/\gamma$  and the average energy per photon is then

$$\langle E \rangle = \frac{\int d\dot{n}\gamma E_0}{\int d\dot{n}} = \frac{\int d\gamma\gamma E_0 P(\gamma)/\gamma}{\int d\gamma P(\gamma)/\gamma} = E_0\langle\gamma^{-1}\rangle^{-1}. \quad (6)$$

We see here that the received energy per unit time is just the sum of the power of the sources, but the number of received photons per unit time in the observer frame has a  $1/\gamma$  dependence.

For unresolved sources then, the effect of the internal kinematics is to introduce a blue-shift. How does this square with the result obtained in the previous section where we found that the effect for resolved sources was a red-shift that, once we allowed for light cone effects, was actually larger than the transverse Doppler effect? To see that the two calculations are consistent, and obtain a useful check of the validity of the light-cone effect, we now show that the resolved-source analysis reproduces the result for unresolved sources, as of course it should, if we introduce a weight per galaxy proportional to its fluence (number of photons per unit time per unit area at the detector). It is sufficient to consider identical isotropic emitters, for which the fluence is  $dn/dt \sim En(E) \sim E^3$  where the extra factor of energy flux as compare to photon flux comes again from the transformation from intervals of time at the source and at the observer.

The number of photons per second received from such a source is proportional to  $1/\gamma^3(1 - \beta\mu')^3$  and therefore the fluence weighted mean observed photon energy should be given by

$$\langle E \rangle = E_0 \frac{\int d\beta \beta^2 \rho_0(\beta) \int d\mu (1 - \beta\mu)\gamma^{-4}(1 - \beta\mu)^{-4}}{\int d\beta \beta^2 \rho_0(\beta) \int d\mu (1 - \beta\mu)\gamma^{-3}(1 - \beta\mu)^{-3}} \quad (7)$$

where the first factor of  $1 - \beta\mu$  is the asymmetry of the observed phase space distribution from the light-cone effect, and where we have assumed that the distribution of velocities is isotropic and have dropped the prime. The integrals are elementary, and we readily find  $\langle E \rangle = E_0/\langle 1/\gamma \rangle$ , fully consistent with the result obtained above. Without the light-cone  $1 - \beta\mu$  term we would have obtained a different result.

For non-relativistic systems with  $\beta^2 \ll 1$  the effect of the internal motions of emitters within unresolved objects is to give a change of energy  $\delta E/E_0 \simeq \langle \beta^2 \rangle/2$  which is a blue-shift and just opposite to the usual transverse Doppler redshift.

## 4 SURFACE BRIGHTNESS MODULATION

In §2 we implicitly assumed that all galaxies are observed and catalogued. But in reality the galaxies in the spectroscopic sample were selected according to their apparent luminosities. As discussed in §3, a galaxy's apparent luminosity depends on its state of motion through the beaming effect which changes the surface brightness and hence luminosity. This results in a bias for the redshifts of the cluster galaxies which are selected for redshift measurement as the surface brightness modulation means that galaxies moving away from us in a given region of space have a higher limit on their intrinsic luminosities than galaxies moving towards us. For the WHH experiment the effect is quite strong, and strongly increasing with cluster redshift, since the flux limit ( $r = 17.8$ ) is only about one magnitude fainter than  $M_*$  even at the minimum redshift limit, so the flux selection limit falls on the steep end of the luminosity function (LF) where small fractional changes in luminosity have a large effect on the number of sources detected.

We then consider the effect on the BCGs. For these the flux limit is irrelevant, but there is a bias because velocities can change the ranking of the two brightest galaxies. This turns out to be almost independent of cluster redshift.

### 4.1 Flux-Limited Galaxies

For low velocities  $\beta \ll 1$  the fractional change of the fluence is  $\Delta\dot{n}/\dot{n} = 3\beta_x$ , but to obtain the observed photon count, we also need to allow for the change in frequency and the limits imposed by the broad-band filter. Combining these, the fractional change in apparent luminosity for a galaxy in a cluster at redshift  $Z$  is  $\Delta l/l = (3 + \alpha(Z))\beta_x$ , where the effective spectral index, for a photon counting detector with response curve  $R(\lambda)$ , is  $\alpha(Z) = -d \ln(\int d\lambda \lambda R(\lambda)/(1+Z)) f_\lambda / d \ln(1+Z)$ . This depends on the details of the galaxy spectral energy distributions (SEDs). Baldry *et al.* (2002) provide an average SED for galaxies in the 2dFGRS which is very similar to that of an Sb galaxy. We expect the average for galaxies in the main spectroscopic sample from SDSS to be very similar. However, this is a luminosity weighted average, whereas what is really needed is a number weighted average. Since lower luminosity galaxies tend to be more active, this would be expected to be bluer and therefore have a smaller spectral index. A further complication is that the WHH sample includes the luminous red galaxy (LRG) sample (Eisenstein *et al.*, 2001) that are redder - though these are relatively few in number. The effective spectral

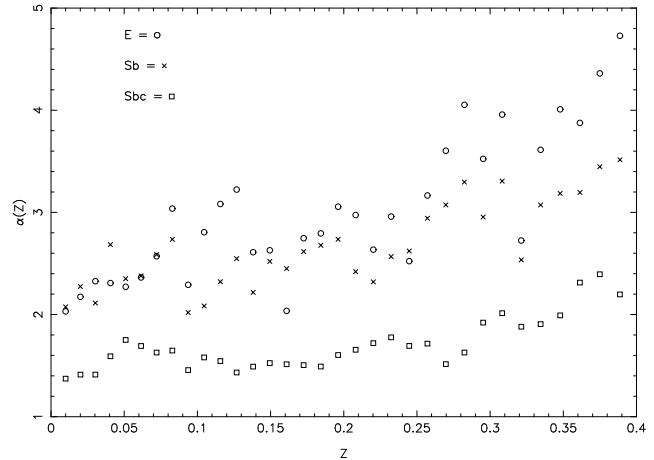


**Figure 1.** Spectral index vs. redshift for representative galaxy types observed in Sloan r-band

indices for representative galaxy types (E, Sb and Sbc) from Coleman, Wu and Weedman (1980) and Kinney *et al.* (1996) are shown in figure 1. At the typical redshift for the sample the spectral index approximately 2.5 for the E and Sb SEDs and about 1.5 for the more active Sbc spectrum. In what follows we shall assume  $\alpha \simeq 2.0$ .

The modulation of the number density of detectable objects is given by the product of  $\Delta l/l$  and the logarithmic derivative  $\delta(Z) \equiv -d \ln n(> L_{\text{lim}}(Z))/d \ln L$  which, as mentioned, is a strongly increasing function of redshift. Ideally we would calculate this using a luminosity function appropriate for the actual cluster galaxies used in the study, and this will, in general, depend on the projected distance from the cluster center. However, Hansen *et al.* (2009) have shown that while the mix of red *vs.* blue galaxies changes strongly with radius, the overall luminosity function does not vary much, and the parameters are not very different from the field galaxy luminosity function, so we will use the latter, as determined for SDSS by Montero-Dorta & Prada (2009), as a proxy. Their estimate of the LF obtained from the r-band magnitudes K-corrected to  $Z = 0.1$  has  $M_* - 5 \log_{10} h = -20.7$  and faint end slope of  $\alpha = -1.26$ . The resulting  $d \ln n(> L)/d \ln L$ , computed using the flux limit  $r = 17.77$  appropriate for the SDSS spectroscopic sample used by WHH, is shown as the dot-dash curve in figure 2. Note that we are ignoring here the contribution from the LRG sample, which are selected according to a more complicated combination of colour and luminosity cuts.

Finally, we need the average of  $-(3 + \alpha)d \ln n(> L)/d \ln L$  over the redshift distribution for the galaxies actually used in the experiment. The 7,800 clusters used by WHH were selected by applying a richness limit to the parent GMBCG catalogue (Hao, J., *et al.* 2010) that contains 55,000 clusters extending to  $Z = 0.55$ . These clusters were derived from the SDSS photometric catalogue that is much deeper than the spectroscopic catalogue. Consequently, at the redshifts where the spectroscopically selected galaxies live, this parent catalogue is essentially volume limited for the clusters used, so the redshift distribution for the cluster members used is essentially the same as that for the redshift distribution for the entire spectroscopic sample, save for the fact that the GMBCG cata-

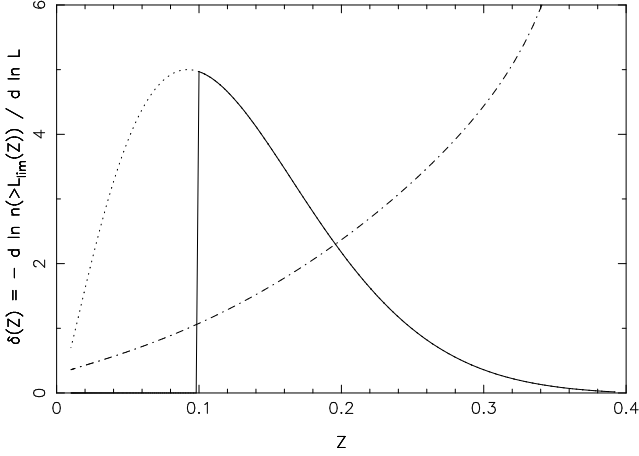


**Figure 2.** The dot-dash curve is the logarithmic derivative of the comoving density of objects above the luminosity limit as a function of redshift. The bell-shaped curve is  $dN/dZ = Z^2 n(Z)$  and the solid curve is that truncated at the minimum redshift imposed by the parent cluster catalogue. The mean of the log-derivative, averaged over the redshift distribution turns out to be  $\simeq 2.0$ .

logue has a lower redshift limit  $Z_{\text{lim}} = 0.1$ , which is very close to the redshift where  $dN/dZ = Z^2 n(Z)$  peaks. This is the bell shaped curve in figure 2. Combining these we find  $\langle d \ln n / d \ln L \rangle = \int dZ Z^2 n(Z) d \ln n / d \ln L / \int dZ Z^2 n(Z) \simeq -2.0$  with integration range  $0.1 < Z < 0.4$ , and the average  $-\langle (3 + \alpha(Z)) d \ln n(> L) / d \ln L \rangle \simeq 10$ . This may be a slight overestimate, as the cluster catalogue is not precisely volume limited and the actual  $dN/dZ$  may lie a little below the solid curve in figure 2 at the highest redshifts.

For the WHH experiment, the surface brightness modulation effect is considerably larger in amplitude than the transverse Doppler and light-cone effects, but has opposite sign. For isotropic orbits the combination of the TD, LC and SB effects is

$$\langle \delta z \rangle = (2.5 - \langle (3 + \alpha(Z)) \delta(Z) \rangle) \langle \beta_x^2 \rangle \simeq -7.5 \langle \beta_x^2 \rangle. \quad (8)$$

## 4.2 Effect on BCGs

The TD and LC effects act on all galaxies, including the BCGs, in the same way. The SB effect is different; in the WHH analysis, only clusters with at least 5 measured redshifts were used, so it is safe to assume that the brightest cluster galaxies will be unaffected by the flux limit. However, for some small fraction of the clusters, the two brightest galaxies will have magnitudes that are sufficiently close that the effect of surface brightness modulation by the motions will be enough to change their ranking, resulting in a bias. In principle, this effect could be eliminated by only using clusters where the difference between the two brightest galaxies is sufficiently large that the velocities cannot change the ranking.

To analyse this, let the joint distribution of difference of intrinsic magnitudes  $m_{ab} = m_a - m_b$ , and line-of-sight velocities  $\beta_a, \beta_b$  for pairs of top two ranked cluster galaxies, in no particular order, be  $P_0(m_{ab}, \beta_a, \beta_b)$ . This is a symmetric function of  $m_{ab}$ .

The velocities change the observed surface brightnesses of the galaxies, and hence the difference of ob-

served magnitudes is  $m'_{ab} = m_{ab} - \kappa(\beta_a - \beta_b)$ , where  $\kappa \equiv (\ln(10)/2.5)(3 + \alpha(Z))$ , so the observed distribution is  $P(m_{ab}, \beta_a, \beta_b) = P_0(m_{ab} - \kappa(\beta_a - \beta_b), \beta_a, \beta_b)$ , the Jacobian of the transformation from intrinsic to observed magnitude being unity.

The probability distribution for the velocity of the first ranked galaxy  $\beta_1$  is then

$$P(\beta_1) = \int_{-\infty}^0 dm_{ab} \int_{-\infty}^{\infty} d\beta_b P(m_{ab}, \beta_1, \beta_b) + \int_0^{\infty} dm_{ab} \int_{-\infty}^{\infty} d\beta_a P(m_{ab}, \beta_a, \beta_1) \quad (9)$$

i.e. the sum of the distribution function for  $\beta_a$  if  $m_{ab} < 0$  and the DF for  $\beta_b$  if  $m_{ab} > 0$ .

Making a Taylor expansion of  $P(m_{ab}, \beta_a, \beta_b)$  with respect to  $m_{ab}$  and performing the integrals yields

$$P(\beta_1) = P_0(\beta_1) - 2\kappa\beta_1 P_0(m_{ab} = 0, \beta_1) \quad (10)$$

which depends on the joint distribution of the intrinsic magnitude difference and the velocity of one or other of the two brightest galaxies. The mean redshift offset is then

$$\langle \delta z_{\text{BCG}} \rangle = -\kappa \sigma_{ab}^2 P_0(m_{ab} = 0) / c^2 \quad (11)$$

where  $\sigma_{ab}^2 \equiv \langle (\beta_a - \beta_b)^2 | m_{ab} = 0 \rangle$  is the variance of the relative velocity of the two brightest galaxies given that they have similar magnitudes. This is something that is straightforward to measure from the data. It is reasonable to expect that this is larger than (twice) the velocity variance for brightest cluster galaxies. Smith *et al.* (2010) have measured the distribution for magnitude differences and find  $P_0(m_{ab} = 0) \simeq 0.35$  so we then have

$$\langle \delta z_{\text{BCG}} \rangle \simeq 0.32(3 + \alpha(Z)) \sigma_{ab}^2 / c^2 \simeq 1.9 \text{ km s}^{-1} / c(\sigma_{ab} / 600 \text{ km/s})^2. \quad (12)$$

Note that the surface brightness boosting effect on BCGs does not have the strong redshift dependence that is expected for the flux-selected galaxies.

## 5 REVISED REDSHIFT PROFILE PREDICTION

We can now make a prediction for the combined GR+TD+LC+SB effect as a function of radius using the observed velocity dispersion data provided by WHH. We first review the relevant properties of the BCGs; both their cluster-centric kinematics and their halo properties. We then attempt to combine all of the effects discussed above to predict the expected profile of the redshift offset and its constituent components. We caution at the outset that there are considerable uncertainties in many of the critical inputs that feed through into the prediction.

### 5.1 Motion of BCGs Within Clusters

The analysis of WHH relies on the assumption that, in an average sense, the BCGs used as the origin of coordinates in velocity and angle space are a relatively cold population, velocity-wise, compared to the other galaxies and are therefore orbiting close to the potential minimum. There are good theoretical grounds for believing that the BCGs will indeed

be colder than the general population, but understanding in detail just how cold they are is important here for two reasons: first because both the gravitational redshift and the kinematically sourced effects depend on the velocity dispersions of the BCGs which, following WHH, must be subtracted in quadrature from the observed dispersion profile, and second because it can inform us to what extent the mean density profile around the BCG is in fact likely to depart from the idealised NFW model predictions if the BCGs do not reside precisely at the minimum of the potential.

WHH assume  $\sigma_{\text{BCG}} = 0.35\sigma_{\text{obs}}$ , citing Skibba *et al.* (2011), in which case the effect on estimates of e.g. the TD and LC effects is quite small. But this may be a bit low. Skibba *et al.* found that the velocity dispersion for the *central* galaxies in the clusters were  $\sigma_{\text{cen}} \simeq 0.5\sigma_{\text{CL}}$  which is a lot larger, but not directly measuring the same thing since they also found that about 30% of the time, the central galaxy was not in fact the brightest galaxy in the cluster.

Coziol *et al.* (2009) have measured the distribution of BCG motions directly and find that  $\langle |v_{\text{BCG}}| \rangle / \sigma_{\text{CL}} \simeq 0.40 \pm 0.04$  for clusters of Abell richness class  $R=1$ . These clusters have mean dispersion  $\sigma = 651$  km/s, a little higher than for the composite cluster here. The mean dispersion for  $R=0$  is  $\sigma = 539$  km/s, for which they find  $\langle |v_{\text{BCG}}| \rangle / \sigma_{\text{CL}} \simeq 0.43 \pm 0.03$  so the appropriate value for the sample here is around 0.42.

For a Gaussian distribution,  $\langle |v_{\text{BCG}}| \rangle = \sqrt{2/\pi}\sigma_{\text{BCG}}$  so this suggests  $\sigma_{\text{BCG}} = 0.53\sigma_{\text{CL}}$  which is again considerably larger than the value adopted by WHH and consistent with what Skibba *et al.* found for the central cluster galaxies.

There is clearly considerable uncertainty in the true value of  $\sigma_{\text{BCG}}$ . In what follows we will assume  $\sigma_{\text{BCG}} = 0.50\sigma_{\text{CL}}$ . If we define  $\alpha \equiv \sigma_{\text{BCG}}^2 / \sigma_{\text{CL}}^2$  then we have  $\sigma_{\text{CL}}^2 = \sigma_{\text{obs}}^2 / (1 + \alpha)$  and  $\sigma_{\text{BCG}}^2 = (\alpha / (1 + \alpha)) \sigma_{\text{obs}}^2$ . For  $\alpha = 0.25$  and  $\sigma_{\text{obs}} = 620$  km/s we have  $\sigma_{\text{BCG}} = 277$  km/s and  $\sigma_{\text{CL}} = 555$  km/s. With this value the differential TD and LC effects are reduced to about 60% of what one would expect in the limit that the BCGs lie at rest at the minimum of the cluster potential. The SB effect, as we show below, is somewhat less affected.

We can also estimate the reduction in the gravitational redshift, assuming that the clusters in which the BCGs live do indeed have NFW profiles. Vanishing of the second time derivative of the moment of inertia  $I = \sum r^2$  tells us that  $\langle |\dot{r}|^2 \rangle = 3\sigma_{\text{BCG}}^2 = \langle r|\nabla\Phi| \rangle$ . In the inner parts of the NFW profile, the potential increases linearly with radius, so consequently we have  $\langle r|\nabla\Phi| \rangle = \langle \Phi \rangle$  so the predicted gravitational blue-shift for the hot population relative to the colder BCG population is decreased by  $\delta z = 3\sigma_{\text{BCG}}^2 / c^2 \simeq 0.9(\sigma_{\text{BCG}} / 300 \text{ km/s})^2 \text{ km s}^{-1}/c$ . But their motions will also give them TD and LC red-shifts that are  $\delta z \simeq 2.5\sigma_{\text{BCG}}^2 / c^2$  which largely counteracts the change in the GR effect, and from §4.2 the SB effect on the BCGs gives them a blue shift which we have estimated to be about  $c\delta z = -1.9$  km/s.

Finally, one should allow for the fact that the light we see from the galaxies will have suffered gravitational redshift escaping the halos of the galaxies, and that the starlight will also be affected by stellar motions as described above in §3. This is most important for the BCGs.

## 5.2 BCG Internal Kinematics and Halo Properties

Regarding the GR effect, the stellar velocity dispersion in BCGs is typically  $\sigma_* \sim 250$  km/s (e.g. Bernardi *et al.*, 2007); much larger than that of the run-of-the-mill galaxies, and quite comparable to the motion of the BCGs in the cluster halo. The BCGs are unresolved, so we can use the result of §3 to predict the kinematically sourced blue-shift  $\delta z \sim -(3/2)(\sigma_*/c)^2 \sim -0.3 \text{ km s}^{-1}/c$ , which is quite small. If they have flat rotation curve halos, for which  $\Phi = \Phi_0 \ln r$  then, for isotropic orbits,  $\Phi_0 = 2\sigma_{DM}^2$  while vanishing of  $\dot{I}$  for the stars requires  $\Phi_0 = 3\sigma_*^2$ . The gravitational redshift is therefore  $\delta z = 3(\sigma_*^2/c^2)\langle \ln(r_{\text{halo}}/r_*) \rangle = 0.63 \text{ km s}^{-1}/c(\sigma_*/250 \text{ km/s})^2 \langle \ln(r_{\text{halo}}/r_*) \rangle$ . The problem here is determining the logarithm since we need to know the size of the BCG halo (as distinct from the cluster halo). This could be determined by galaxy-galaxy lensing, and also could in principle be determined from simulations.

A rough estimate can be obtained from tidal considerations: The BCG halo density is  $\rho_{\text{halo}} \sim 3\sigma_*^2/4\pi Gr_{\text{halo}}^2$  while the density of the cluster is  $\rho_{\text{CL}} \sim 2\sigma_{\text{CL}}^2/4\pi Gr^2$  where now  $r$  is the typical cluster-centric distance to the BCG. If this is a few hundred kpc then the tidal constraint that  $\rho_{\text{halo}} \geq \rho_{\text{CL}}$  says that  $r_{\text{halo}}$  can't be bigger than about 1/3 of this. The scale lengths for BCGs are typically 10kpc, so this would suggest that the logarithm is approximately 2.5. If the halos are really this large, the effect of the motion of the stars  $\delta z \simeq -3\sigma_*^2/2c^2$  is a small correction, and we have a net redshift  $\delta z \simeq 1.25 \text{ km s}^{-1}/c$ .

## 5.3 Combined Prediction

We will proceed in two steps. We bootstrap off the estimate of the difference in potential between the BCG and the innermost point using the WHH stacked NFW model method. The innermost data point lies at  $r_{\perp} = 0.6$  Mpc where the assumptions of virial equilibrium are likely to be well obeyed. We then extrapolate to larger impact parameters assuming galaxies trace the mass and using the cluster-galaxy cross-correlation function to get the appropriate ensemble average mass profile.

The stacked NFW model appears to provide a good fit to the data within 1.2 Mpc (WHH supplementary figure 2) and yields a potential for galaxies at impact parameter 0.6 Mpc corresponding to  $\delta z_{\text{GR}} \simeq -5.0 \text{ km/s/c}$ . The finite BCG velocities will reduce the gravitational potential difference by about  $0.9 \text{ km/s/c}$  but the BGH halo potential increases it by an estimated  $1.6 \text{ km/s/c}$ . The net result is a potential difference of  $\delta z_{\text{GR}}(0.6 \text{ Mpc}) \simeq -5.7 \text{ km/s/c}$ .

We now need include the kinematic effects. The observed velocity dispersion at this impact parameter is  $\sigma_{\text{obs}} \simeq 620$  km/s, so with  $\sigma_{\text{BCG}} = 0.5\sigma_{\text{CL}}$  the LC and TD effects are  $\delta z_{\text{TD+LC}} \simeq (3/5)2.5\sigma_{\text{obs}}^2/c^2 = +1.9 \text{ km s}^{-1}/c$ . The SB effect for the non-BCGs is  $\delta z_{\text{SB}} \simeq -10.0\sigma_{\text{CL}}^2/c^2 \simeq -10.3 \text{ km s}^{-1}/c$  and the SB effect on the BCGs we have estimated to be about  $+1.9 \text{ km s}^{-1}/c$ , and finally the kinematic blue-shift for the stars in the BCG gives  $+0.3 \text{ km s}^{-1}/c$  for a net kinematic effect  $\delta z_{\text{TD+LC+SB}}(0.6 \text{ Mpc}) \simeq -6.1 \text{ km s}^{-1}/c$  for a grand total  $\delta z_{\text{GR+TD+LC+SB}}(0.6 \text{ Mpc}) \simeq -11.8 \text{ km s}^{-1}/c$ . whereas the observed value is  $\delta z \simeq -2.6 \text{ km s}^{-1}/c$ . The uncertainty on this point is approximately  $6 \text{ km s}^{-1}/c$  so this

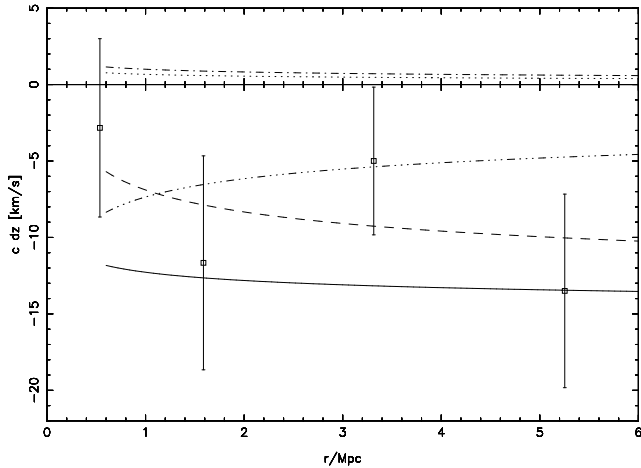


**Figure 3.** Data points from figure 2 of WHH and prediction based on mass-traces-light cluster halo profile and measured velocity dispersions as described in the main text. The dashed line is the gravitational redshift prediction, which is similar to the WHH model prediction. The dot-dash line is the transverse Doppler effect. The dotted line is the LC effect. The triple dot-dash line is the surface brightness effect. The solid curve is the combined effect.

would appear to be discrepant, but only at about the 1.5-sigma level.

The NFW model predicts  $\delta z \simeq -10 \text{ km s}^{-1}/c$  for the outer measurements  $r \simeq 3.3, 5.3 \text{ Mpc}$ , and the measurements straddle this value. While this model may provide a reasonable description for isolated clusters in the virialised domain, it is not at all clear that it is appropriate to describe the composite cluster being studied here. Tavio *et al.* (2008) have claimed that beyond the virial radius the density in numerical LCDM simulations actually falls off like  $\rho \sim 1/r$  rather than the  $\rho \sim 1/r^3$  asymptote for the NFW profile, and the extended peculiar in-fall velocities found by Ceccarelli *et al.* (2011) also argue for shallow cluster profiles, but it is not clear that these results are widely accepted.

An alternative, and possibly more reliable, approach is to assume that galaxies trace the mass reasonably well, in which case the density profile of the stacked cluster has the same shape as the cluster-galaxy cross correlation function (e.g. Lilje & Efstathiou, 1988; Croft *et al.*, 1997). This has a power-law dependence  $\rho \sim r^{-\gamma}$  with  $\gamma \simeq 2.2$ , i.e. intermediate between the NFW and Tavio *et al.* model predictions.

For space density  $\rho(r) = \rho_0(r/r_0)^{-\gamma}$ , where  $r_0$  is an arbitrary fiducial radius, the potential is  $\Phi(r) = \Phi_0(r/r_0)^{2-\gamma}$  and the 1-D velocity dispersion, for isotropic orbits, is  $\sigma^2(r) = \sigma_0^2(r/r_0)^{2-\gamma}$  with  $\Phi_0 = 2((1-\gamma)/(2-\gamma))\sigma_0^2$ .

The projected velocity dispersion measured is related to the 3-D velocity dispersion by  $\sigma^2(r_\perp)/\sigma^2(r) = \int dy y^{2-\gamma}(1+y^2)^{-\gamma/2}$  but the projected potential is related to the 3-D potential in the same way, so the projected quantities are related by  $\Phi(r_\perp) = 2((1-\gamma)/(2-\gamma))\sigma^2(r_\perp)$ . This is the potential relative to infinity. The difference in projected potential between two projected radii  $r_1$  and  $r_2$  is  $\Phi(r_2) - \Phi(r_1) \simeq 12\sigma^2(r_1)(1 - (r_1/r_2)^{0.2})$  for  $\gamma = 2.2$ . The resulting GR effect is shown as the dashed line in figure 3 and is actually quite similar to the shape of the profile for the WHH NFW composite model.

The FWHM of the bell-shaped velocity distributions in

WHH figure 1 appear to decrease by about 15% between the inner-bin and the outer points. This is reasonably consistent with the expected  $\sigma^2 \propto r^{-0.2}$  trend predicted if galaxies trace mass, but this is perhaps fortuitous since the outer points are well outside the virial radius. Regardless of whether the galaxies at large radius are equilibrated or not, we can use the change in the observed velocity dispersion with radius to obtain the differential TD+LC+SB effect which is shown, added to the GR effect, as the solid line in figure 3. The kinematic effects flatten out the predicted profile, so the prediction is quite different from the gravitational redshift alone.

The situation is clearly rather complicated, especially when using BGCs as the origin of coordinates since the effects depend on things like the relative velocities of the top ranked pair of cluster galaxies, and on the BCG halo properties, that are quite poorly known. However, those factors only influence the prediction for the innermost data point. The empirically based theoretical prediction for the profile of the redshift offset for the hot population as a function of impact parameter at  $r_\perp > 0.6 \text{ Mpc}$  is the most robust; if galaxies are reasonable tracers of the mass then profile should be very flat, quite unlike the GR effect from a NFW profile. The predicted GR and total effects are shown in figure 3. However, this analysis ignores the effect of secular infall and out-flow which we consider next.

## 6 EFFECT OF INFALL AND OUTFLOW

The discussion so far has focused mostly on the stable, virialised regions. Clusters, however, are evolving structures and the mass within any fixed physical radius  $M(r)$  will in general be changing. Outside of the virial radius (generally considered, inspired by the spherical collapse model, to be the radius within which the mean enclosed mass density is  $3\pi/Gt^2$ ) we expect to see net infall, and the enclosed mass at those radii will be increasing with time, while at still larger radii there will be outflow tending asymptotically toward the Hubble flow. In the spherical collapse model the transition from inflow to outflow takes place at the turnaround radius where the mean enclosed mass density is  $\bar{\rho}_t = 3\pi/32Gt^2$ . This is for a matter dominated Universe; allowing for a cosmological constant makes only a small change (Lokas & Hoffmann, 2001).

For the empirically motivated  $\rho = \rho_0(r/r_0)^{-\gamma}$  model the mean enclosed mass is  $\bar{\rho}(r) = 3(\gamma - 1)(2\pi G)^{-1}\sigma_0^2 r_0^{\gamma-2} r^{-\gamma}$  and the nominal virial radius is  $r_{\text{vir}} = ((\gamma - 1)\sigma_0^2 r_0^{\gamma-2} t^2 / 2\pi^2)^{1/\gamma} \simeq 1.8 \text{ Mpc}$  using  $\gamma = 2.2$ ,  $r_0 = 1 \text{ Mpc}$ ,  $\sigma_0 = 545 \text{ km/s}$  and  $t \simeq 1/H = 1/(70 \text{ kms}^{-1}/\text{Mpc})$  and turnaround is at  $r_t \simeq 8.7 \text{ Mpc}$ .

In the centres of clusters there may be softening of the cores which would reduce the enclosed mass and would have an associated outflow.

In any single cluster, the density may be changing rapidly — on the local dynamical timescale — especially during mergers and as clumps rain in, but for a composite cluster such as considered here these rapid changes will average out and the mass can only change on a cosmological timescale:  $\dot{M} \sim HM$ . For power law profile with  $\gamma \simeq 2$   $M \simeq 4\pi\rho r^3$  and  $\dot{M} \simeq 4\pi\rho r^2\bar{v}$ , where  $\bar{v}$  is the mean infall ve-

locity, by continuity. So if  $\dot{M}(r) = \alpha(r)HM(r)$ , with, by the above argument,  $\alpha(r)$  of order unity, then  $\nabla(\mathbf{r}) = \alpha(r)H\mathbf{r}$ .

This secular flow can generate a net offset for the redshifts in two ways. First, and most importantly for clusters at  $Z \ll 1$ , along any line of sight we observe galaxies that lie in a cone that will be wider at the back of the cluster. At low redshift this means there will be more galaxies observed at the back than the front in an intrinsically symmetric cluster. But we also need to allow for the countervailing bias caused by the fact that the more distant galaxies will be fainter which, as we have seen above, overwhelms the effect of the change of volume in the relevant range of redshifts. These geometric and flux limit effects, whose effects on the foreground and background galaxies was discussed by Kim and Croft (2004), modulate the density per unit line of sight distance linearly with distance. The real flux limited galaxies observed along cones behave like particles with no flux selection observed in cylinders with a phase space density  $\rho'(\mathbf{r}, \beta) = \rho(\mathbf{r}, \beta)(1 + 2Hx(\delta(Z) - 1)/cZ)$ .

We can try to use this to estimate the redshift offset as  $\int dx \int d^3\beta \rho'(\mathbf{r}, \beta) \beta_x / \int dx \int d^3\beta \rho(\mathbf{r}, \beta)$ . Performing the integrals over velocity this is

$$\langle \beta_x \rangle_{r_\perp} = \int dx \left( 1 + \frac{2Hx}{cZ} (\delta(Z) - 1) \right) \rho(\mathbf{r}) \bar{\beta}_x(\mathbf{r}) / \int dx \rho(\mathbf{r}) \quad (13)$$

or, with  $\bar{\beta}_x(\mathbf{r}) = \alpha(r)Hx/c$  and an assumed  $\sim 1/r^2$  density profile,

$$\langle \beta_x \rangle_{r_\perp} = \frac{2H^2}{c^2 Z} (\delta(Z) - 1) \int dx \frac{\alpha(r)x^2}{r^2} / \int \frac{dx}{r^2} \quad (14)$$

where  $r = \sqrt{r_\perp^2 + x^2}$ . This is rather messy and, owing to the presence of the factor  $\alpha(r)$ , model dependent. But we can note the following: if we work at  $r_\perp \sim 1\text{Mpc}/h$  say, the integral in the denominator will be  $\sim 1/r_\perp$  while the contribution to the integral in the numerator from  $-r_\perp < x < r_\perp$  will be  $\sim r_\perp \alpha(r_\perp)$ , so we get a partial contribution to  $\langle \beta_x \rangle_{r_\perp} \sim H^2 r_\perp^2 / c^2 Z \simeq 5 \times 10^{-7} Z_{0.2}^{-1}$ , which is very small; corresponding to a physical velocity of only 0.16 km/s. If we extend the range of integration beyond  $|x| < r_\perp$  this will increase, but not by a very large factor, since  $\alpha(r)$  will start its decrease towards zero at the turnaround radius. Extending the range of integration still further the average decreases since  $\alpha$  now has changed sign. Ultimately, the value of this integral will become large, and even more so beyond the  $\sim 10\text{Mpc}/h$  scale of the cluster-galaxy cross-correlation function, but this would not be seen as a shift of the bell-shaped enhancement of the redshift distribution.

The secular infall or outflow can also couple to the time rate of change of the phase space distribution function, which will also be changing on a cosmological timescale (both the density and the width of the velocity distribution will, in general, be varying). This will result in a formally similar contribution to the redshift offset, but without the factor  $1/Z$ , so for low-redshift clusters this will be still smaller.

At larger impact parameter the effect of outflow is more interesting. In figure 3 we show the line-of-sight velocity distribution for a simple, but plausible, model for cluster density and velocity structure in the out-flow region. The key assumption here is that outside of turnaround the radial velocity is  $v \simeq H(r - r_t)$  and is supported by the analysis of peculiar velocity profiles numerical simulations (Cec-

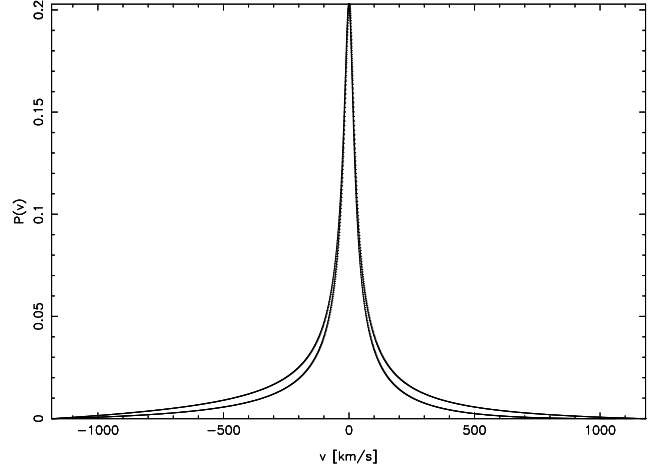


**Figure 4.** Distribution of line of sight velocities at impact parameter  $r_\perp = 10\text{Mpc}$  for a simple model where  $\xi_{\text{cg}} = (r/r_0)^{-2}$  with correlation length  $r_0 = 10\text{Mpc}$  and turnaround radius  $r_t = 8.7\text{Mpc}$  and where the velocity is  $v = H(r - r_t)$ . A linear ramp determined from the outermost points has been subtracted. These were generated using equation 13 with parameter  $2H(\delta(Z) - 1)/cZ = 0$  (thin line) and  $0.023/\text{Mpc}$  (thick line). This is highly exaggerated. For clusters at  $Z = 0.2$ , or averaged over the distribution of galaxy redshifts, this parameter is  $\simeq 0.0023$ . Scaling the mean velocity appropriately gives  $\delta z \simeq -3.0 \text{ km s}^{-1}/c$ . This is for cold spherical outflow. In reality this will be convolved with a broad quasi-Gaussian distribution of random velocities from local substructures but the shift of the centroid will be essentially the mean of the distribution shown here.

carelli, *et al.*, 2011). The amplitude of the effect has been exaggerated in figure 4 by a factor 10 for clarity. For the average of  $2H(\delta(Z) - 1)/cZ$  over the distribution of galaxy redshifts shown in figure 2 is approximately  $0.0023/\text{Mpc}$ . Scaling the mean velocity from the model appropriately yields an expected blue-shift driven by the out-flow of about  $\delta z \simeq -3.0 \text{ km s}^{-1}/c$  at impact parameter  $r_\perp \simeq 10\text{Mpc}$ . Over the range of impact parameters explored by WHH the effect of infall and outflow is very small.

## 7 DISCUSSION

We have shown that, in addition to the transverse Doppler effect, there are additional factors that need to be taken into account in interpreting the measurement of the offset of the net blue-shift of the cluster galaxies relative to the central brightest cluster galaxy. These are straightforward to estimate from the measured line-of-sight velocities and can therefore be subtracted from the measured blue-shift. The TD effect is a little more difficult to estimate, as it depends to some degree on the velocity dispersion anisotropy, but as it is a relatively small effect for the WHH experiment little error is made if we assume isotropic orbits. We have also shown that the redshift offset for unresolved sources is different again; the kinematically sourced effect is a blue-shift that is just the opposite of the standard transverse Doppler term.

We have applied these results to the WHH measurement. We have used an empirically motivated model for the composite cluster halo mass density profile together with the



observed velocity dispersions to predict the net redshift offset. The largest correction comes from the surface brightness modulation effect. This is roughly equal to the GR effect at small impact parameters, and, since the velocity dispersion is falling with radius, this flattens out the blue-shift profile. The result, it has to be admitted, does not seem to agree as well with the data as the GR prediction alone.

The current data do not place particularly strong constraints on theories that invoke long-range non-gravitational interactions in the dark sector. However, the observational situation has already improved substantially with nearly three times as many galaxy redshifts obtained by the Sloan telescope once one includes the extensions such as BOSS (Dawson *et al.*, 2013), and in the near future there will be yet more data available, from surveys such as big-BOSS and also potentially from ASKAP and Aperitif in the radio (Duffy, *et al.*, 2012), to strengthen this test of fundamental physics.

## 8 ACKNOWLEDGEMENTS

The author enjoyed stimulating discussions on this subject with Bob McLaren, Pat Henry, Harald Ebeling, William Burgett, Bill Unruh, Richard Ellis, and Alex Szalay, and is particularly grateful for useful input from Scott Tremaine and John Peacock. This study was aided by the support of Cifar.

## REFERENCES

- Abazajian K. N., et al., 2009, ApJS, 182, 543  
 Baldry I. K., et al., 2002, ApJ, 569, 582  
 Bekenstein J. D., 2004, PhRvD, 70, 083509  
 Bekenstein J. D., Sanders R. H., 2012, MNRAS, 421, L59  
 Bernardi M., Hyde J. B., Sheth R. K., Miller C. J., Nichol R. C., 2007, AJ, 133, 1741  
 Binney J., Tremaine S., 2008, Galactic Dynamics, 2nd Ed., Princeton University Press  
 Broadhurst T., Scannapieco E., 2000, ApJ, 533, L93  
 Bunn E. F., Hogg D. W., 2009, AmJPh, 77, 688  
 Cappi A., 1995, A&A, 301, 6  
 Ceccarelli L., Paz D. J., Padilla N., Lambas D. G., 2011, MNRAS, 412, 1778  
 Coleman G. D., Wu C.-C., Weedman D. W., 1980, ApJS, 43, 393  
 Coziol R., Andernach H., Caretta C. A., Alamo-Martínez K. A., Tago E., 2009, AJ, 137, 4795  
 Croft R. A. C., Dalton G. B., Efstathiou G., Sutherland W. J., Maddox S. J., 1997, MNRAS, 291, 305  
 Dawson K. S., et al., 2013, AJ, 145, 10  
 Duffy A. R., Meyer M. J., Staveley-Smith L., Bernyk M., Croton D. J., Koribalski B. S., Gerstmann D., Westerlund S., 2012, MNRAS, 426, 3385  
 Dunkel J., Hänggi P., Hilbert S., 2009, NatPh, 5, 741  
 Eisenstein D. J., et al., 2001, AJ, 122, 2267  
 Farrar G. R., Rosen R. A., 2007, PhRvL, 98, 171302  
 Gradwohl B.-A., Frieman J. A., 1992, ApJ, 398, 407  
 Gubser S. S., Peebles P. J. E., 2004, PhRvD, 70, 123511  
 Hansen S. M., Sheldon E. S., Wechsler R. H., Koester B. P., 2009, ApJ, 699, 1333  
 Hao J., et al., 2010, ApJS, 191, 254  
 Kasun S. F., Evrard A. E., 2005, ApJ, 629, 781  
 Kim Y.-R., Croft R. A. C., 2004, ApJ, 607, 164  
 Kinney A. L., Calzetti D., Bohlin R. C., McQuade K., Storchi-Bergmann T., Schmitt H. R., 1996, ApJ, 467, 38

- Lilje P. B., Efstathiou G., 1988, MNRAS, 231, 635  
 Lokas, E. L., Hoffman, Y., 2001, in proceedings Identification of Dark Matter, eds. Spooner, N. J. C. and Kudryavtsev, V., arXiv:astro-ph/0011295  
 Lynden-Bell D., 1967, MNRAS, 136, 101  
 Montero-Dorta A. D., Prada F., 2009, MNRAS, 399, 1106  
 Navarro J. F., Frenk C. S., White S. D. M., 1997, ApJ, 490, 493  
 Skibba R. A., van den Bosch F. C., Yang X., More S., Mo H., Fontanot F., 2011, MNRAS, 410, 417  
 Smith G. P., et al., 2010, MNRAS, 409, 169  
 Tavio H., Cuesta A. J., Prada F., Klypin A. A., Sanchez-Conde M. A., 2008, arXiv:0807.3027  
 Will, C.M., 2006, Living Reviews of Relativity, 9, 3  
 Wojtak R., Hansen S. H., Hjorth J., 2011, Nature, 477, 567  
 Zhao, H., Peacock, J.A., Li, B., 2012. arXiv:1206.5032

## APPENDIX A: PREDICTING THE REDSHIFT DISTRIBUTION

We have estimated above the effects on the mean redshift. However, what is actually measured is not a simple centroid, since there are foreground and background galaxies so what WHH did was to fit the distribution of redshifts relative to the BDG to a model with a background consisting of a linear ramp and a cluster consisting of a double Gaussian. Given a theoretical model for the PSD, either analytic or obtained by stacking clusters found in a simulation, one would like to generate the predicted distribution of redshifts as a function of impact parameter. A convenient way to do this is to note that the observed redshift  $z$  expressed as a recession velocity is, as before,  $\beta'_x = -z = \beta_x - \beta_x^2/2 - \beta_\perp^2/2 + \Phi/c^2$ , where we have now separated  $\beta^2$  into line of sight and transverse components. Thus  $d\beta'_x = (1 - \beta_x)d\beta_x$ ; i.e. the Jacobian of the transformation from velocity  $\beta$ , with respect to the rest-frame observers, to measured redshift  $\beta'$  is  $1 - \beta_x$ . Conservation of particles requires that the observed density of particles as a function of position, redshift and transverse velocity  $\rho'(\mathbf{r}, \beta'_x, \beta_\perp)$  satisfies  $\rho'(\mathbf{r}, \beta'_x, \beta_\perp)d\beta'_x = \rho_{LC}(\mathbf{r}, \beta_x, \beta_\perp)d\beta_x$  so

$$\rho'(\mathbf{r}, \beta'_x, \beta_\perp) = \rho_{RF}(\mathbf{r}, \beta'_x + \beta_x^2/2 + \beta_\perp^2/2 - \Phi/c^2, \beta_\perp) \quad (\text{A1})$$

i.e. the density of objects in position, radial and transverse velocities is a mapping of the rest-frame PSD with a displacement along the  $\beta_x$  axis. Note that  $\beta_\perp^2$  here denotes the sum of the squares of the two transverse velocity components.

We can now expand the RHS as a Taylor series for small displacement. We also want to evaluate this at  $t = x/c$ , which we can also treat as a small displacement, resulting in

$$\begin{aligned} \rho'(\mathbf{r}, \beta_x, \beta_\perp) &= \rho(\mathbf{r}, \beta_x, \beta_\perp) \\ &+ (\beta_x^2/2 + \beta_\perp^2/2 - \Phi/c^2) \frac{\partial \rho(\mathbf{r}, \beta_x, \beta_\perp)}{\partial \beta_x} \\ &+ \frac{x}{c} \dot{\rho}(\mathbf{r}, \beta_x, \beta_\perp) \end{aligned} \quad (\text{A2})$$

where dot denotes partial derivative with respect to time, and we have dropped the prime on  $\beta_x$ . Integrating over the

transverse velocity components gives

$$\begin{aligned}\rho'(\mathbf{r}, \beta_x) &= \rho(\mathbf{r}, \beta_x) \\ &+ (\beta_x^2/2 + \langle \beta_\perp^2 \rangle/2 - \Phi/c^2) \frac{\partial \rho(\mathbf{r}, \beta_x)}{\partial \beta_x} \\ &+ \frac{x}{c} \dot{\rho}(\mathbf{r}, \beta_x).\end{aligned}\quad (\text{A3})$$

As a sanity check, if we ignore the last term, multiply by  $\beta_x$ , and integrate over space and velocity, assuming  $\rho$  to be an even function of its arguments, we find  $\delta z = \langle -\beta_x \rangle = \langle \beta_x^2 \rangle + \langle \beta_x^2 + \beta_\perp^2 \rangle/2 - \Phi/c^2$  in accord with equation (5).

We could integrate this expression over line of sight distance to get the distribution function for the observed redshift as a function of the impact parameter, but that would not properly allow for the fact that we observe in a cone, nor would it incorporate the surface brightness boosting effects. Both of these can be allowed for simply by multiplying the first term on the RHS by the factors  $1 + (3 + \alpha(Z))\delta(Z)\beta_x$  and  $1 + 2Hx(\delta(Z) - 1)/cZ$ . Linearising the result gives:

$$\begin{aligned}\rho'(\mathbf{r}_\perp, \beta_x) &= \rho(\mathbf{r}_\perp, \beta_x) + \int dx \{ \\ &(\beta_x^2/2 + \langle \beta_\perp^2 \rangle/2 - \Phi/c^2) \frac{\partial \rho(\mathbf{r}, \beta_x)}{\partial \beta_x} \\ &+ ((3 + \alpha(Z))\delta(Z)\beta_x + 2Hx(\delta(Z) - 1)/cZ) \rho(\mathbf{r}, \beta_x) \\ &+ \frac{x}{c} \dot{\rho}(\mathbf{r}, \beta_x) \}.\end{aligned}\quad (\text{A4})$$

This is valid for an individual cluster. If we average over the population of clusters and denote averaged properties as e.g.  $\bar{\rho} = \int dCP(C)\rho / \int dCP(C)$  then we have

$$\begin{aligned}\bar{\rho}'(\mathbf{r}_\perp, \beta_x) &= \bar{\rho}(\mathbf{r}_\perp, \beta_x) + \int dx \{ \\ &\frac{\beta_x^2}{2} \frac{\partial \bar{\rho}(\mathbf{r}, \beta_x)}{\partial \beta_x} + \frac{\partial}{\partial \beta_x} (\langle \beta_\perp^2 \rangle/2 - \Phi/c^2) \bar{\rho}(\mathbf{r}, \beta_x) \\ &+ ((3 + \alpha(Z))\delta(Z)\beta_x + 2Hx(\delta(Z) - 1)/cZ) \bar{\rho}(\mathbf{r}, \beta_x) \\ &+ \frac{x}{c} \dot{\bar{\rho}}(\mathbf{r}, \beta_x) \}.\end{aligned}\quad (\text{A5})$$

The above formulae are valid in the limit  $Z \ll 1$ . The extension to higher redshift is straightforward: Replace  $1/Z \rightarrow d \ln D_A / d \ln(1 + Z)$ . However this is only valid if galaxies are assumed to be non-evolving; in reality evolution will introduce corrections of similar magnitude.

With an ensemble average cluster PSDF, along with the average of this times  $\langle \beta_\perp^2 \rangle/2 - \Phi/c^2$  from e.g. a cosmological simulation, this expression, after integrating along the line-of-sight, provides the predicted distribution function for the observed redshifts which can then be analysed in precisely the same way at the real data (e.g. finding the shift of the velocity distribution by modelling) to obtain the predicted redshift offset as a function of impact parameter. This would also allow comparison of predicted and observed higher order moments of the velocity distribution such as skewness and kurtosis.